Hepatocellular carcinoma cell-specific peptide ligand for targeted drug delivery

Albert Lo,[1,2] Chin-Tarng Lin,[2,3] and Han-Chung Wu[1,2]

[1]Institute of Cellular and Organismic Biology, Academia Sinica; [2]Institute of Pathology, College of Medicine, National Taiwan University; and [3]Department of Pathology, National Taiwan University Hospital, Taipei, Taiwan

Abstract

Hepatocellular carcinoma is the fourth leading cause of cancer death worldwide. Novel treatment strategies derived from increased knowledge of molecular oncology are constantly being developed to cure this disease. Here, we used phage display to identify a novel peptide (SP94), which binds specifically to hepatocellular carcinoma cells. *In vitro*, the phage clone PC94 was shown to bind to hepatocellular carcinoma cell lines by ELISA and flow cytometry analysis. *In vivo*, PC94 homed specifically to tumor tissues but not to normal visceral organs in severe combined immunodeficient mice bearing human hepatocellular carcinoma xenografts. This homing ability could be competitively inhibited by synthetic peptide, SP94. Immunohistochemical staining confirmed that PC94 localized to tumor tissues and that it could not be detected in SP94-competed tumor tissues. In addition, PC94 recognized the tumor tissue but not nontumor tissue in surgical specimens from hepatocellular carcinoma patients, with a positive rate of 61.3% (19 of 31). With the conjugation of SP94 and liposomal doxorubicin, the targeted drug delivery system enhanced the therapeutic efficacy against hepatocellular carcinoma xenografts through enhanced tumor apoptosis and decreased tumor angiogenesis. Our results indicate that SP94 has the potential to improve the systemic treatment of patients with advanced hepatocellular carcinoma. [Mol Cancer Ther 2008;7(3):579–89]

Received 12/3/07; accepted 1/4/08.

Grant support: Academia Sinica and National Science Council Taiwan grant NSC-96-2323-B-001-002 (H-C. Wu).

The costs of publication of this article were defrayed in part by the payment of page charges. This article must therefore be hereby marked *advertisement* in accordance with 18 U.S.C. Section 1734 solely to indicate this fact.

Note: A. Lo and C-T. Lin contributed equally to this work.

Requests for reprints: Han-Chung Wu, Institute of Cellular and Organismic Biology, Academia Sinica, 128 Academia Road, Section 2, Nankang, Taipei 11529, Taiwan. Phone: 886-2-2789-9558; Fax: 886-2-2785-8059. E-mail: hcw0928@gate.sinica.edu.tw

doi:10.1158/1535-7163.MCT-07-2359

Introduction

On a worldwide basis, hepatocellular carcinoma is the 10th most deadly cancer-related killer. Even with the advances in combinations of surgery, radiation, and chemotherapy, the prognosis for hepatocellular carcinoma remains poor (1). The 5-year survival rate for individuals with liver cancer in the United States is only 8.9% despite aggressive conventional therapy, marking this malignancy the second most lethal cancer after pancreatic ductal adenocarcinoma (4.4% survival at 5 years; ref. 2). In 2005, there were >667,000 new cases of liver cancer worldwide with 80% in Asia and sub-Saharan Africa (3). With tremendous progress in the field of molecular oncology, novel treatment strategies are constantly being developed in attempts to cure this disease.

The development of targeted therapeutics against cancer, with improved discrimination between tumor cells and nonmalignant counterparts, is one of the major goals of current anticancer research. Most chemotherapeutic agents do not preferentially accumulate at the tumor sites. Indeed, the dose that reaches the tumor may be as little as 5% to 10% of the dose accumulating in normal organs (4). The toxic side effects often limit dose escalation of anticancer drugs, leading to incomplete tumor response, early disease relapse, and, ultimately, the development of drug resistance. Several approaches were developed to improve the selective toxicity of anticancer drugs such as encapsulating anticancer drugs in delivery systems (5) and targeting anticancer drugs via monoclonal antibodies (6, 7) or peptide ligands (8, 9) that bind to antigens or receptors that are overexpressed or uniquely expressed on the cancer cells.

Drug delivery systems (DDS) such as lipid- or polymer-based anticancer nanomedicines have been proposed to improve the pharmacologic and therapeutic properties of cytotoxic drugs (10). DDS usually refers to nanoparticles and microparticles with diameters of ≤200 nm, including liposomes and other lipid-based carriers such as micelles, lipid emulsions, and lipid-drug complexes; also included are polymer-drug conjugates and various ligand-targeted products such as immunoconjugates (11). The hyperpermeability of tumor vasculature is one of the key factors governing the successful targeting of a tumor by polymer-based cancer therapies (12). After i.v. administration, the ''leakiness'' of the angiogenic tumor vasculature, estimated to have an average pore size of 100 to 600 nm (13), allows selective extravasation of the conjugate in the tumor tissue. Additionally, tumor tissue frequently lacks effective lymphatic drainage, which subsequently promotes polymer retention. The combination of these factors leads to an accumulation of the conjugate in tumor tissue—a passive targeting phenomenon named by Maeda as the ''enhanced permeability and retention effect'' (14).

Enhanced permeability and retention–mediated passive tumor targeting by liposomes can result in several-fold increases of drug concentration in solid tumors relative to those obtained with free drugs (15).

The particular strength of DDS is their ability to alter the pharmacokinetics and biodistribution of their associated therapeutics (5). The coupling of polyethylene glycol (PEG) or other inert polymers to a variety of therapeutic molecules decreases drug clearance by the kidneys and by the reticular endothelial system (16). For larger particulate carriers, such as liposomes and polymer-drug conjugates, the size of the carrier (generally 50-200 nm in diameter) confines it mainly to the blood compartment, with less pernicious effects on normal organs.

The majority of the DDS currently approved for parenteral administrations include liposomal or lipid-based formulations and therapeutic molecules linked to PEG, for instance, PEGylated liposomal doxorubicin, which has been used to treat highly angiogenic tumors such as AIDS-related Kaposi's sarcoma, with overall response rates of 43% and 59% (17, 18). However, particulate DDS cause increased accumulation of drugs in mononuclear phagocytic system cells in the liver, spleen, and bone marrow, and the possibility exists for increased toxicities to these tissues (19). Moreover, with the increased circulation time and confinement of the particulate DDS, hematologic toxicities such as neutropenia, thrombocytopenia, and leucopenia have also become apparent (20). Thus, efforts are being made to enhance the site-specific actions of DDS by combining them with ligands targeted to tumor cells and tumor vasculature surface antigens or receptors, a process called active- or ligand-mediated targeting (8, 21). In addition, the delivery of chemotherapeutic drugs to tumor tissue through affinity targeting may overcome another obstacle in cancer therapy caused by high tumor interstitial fluid pressure (22, 23).

Although monoclonal antibodies have shown clinical potential as tumor targeting agents, poor tumor penetration of the antibodies due to their size and liver/bone marrow toxicity caused by nonspecific antibody uptake are the two major limitations of antibody therapy. Peptide-targeting agents were proposed to ease the problems associated with antibody cancer therapy (24). Combinatorial libraries displayed on microorganisms have been successfully used to discover cell surface–binding peptides and have thus become an excellent strategy to identify tumor-specific targeting ligands.

Phage display technology has been applied to identify B-cell epitopes (25–27) and discover tumor cells (8, 28, 29) and tumor vasculature-specific peptides (30–33). Combining DDS with tumor-specific peptides, the use of targeted DDS can lead to up to several thousand anticancer drug molecules delivered to tumor cells via only a few targeting ligand molecules. The sustained release of the anticancer drug molecules at the tumor site may also have therapeutic advantages (8, 34). In this study, we describe the identification of a novel hepatocellular carcinoma targeting peptide, SP94, which has clinical potential as a drug delivery guider in the treatment of hepatocellular carcinoma.

Materials and Methods

Cell Lines and Cell Culture

59T, Changliver, HA22T, Hep3B, HepG2, J5, NTUBL, Mahlavu, and SKHep1, which are all human hepatocellular carcinoma lines, and NNM, human primary normal nasomucosal epithelial cells (8), were used in this study. Hepatocellular carcinoma cells were obtained courtesy of Dr. M. Hsiao (Genomic Research Center, Academia Sinica). All the human hepatocellular carcinoma cell lines and NNM were maintained in DMEM and 10% fetal bovine serum at 37°C in a humidified atmosphere of 5% or 10% CO_2 in air.

Phage-Displayed Random Peptide Libraries and Biopanning

Phage-displayed random peptide libraries (Ph.D.-12 kit; New England Biolabs) were employed in our experiments. Biopanning procedures were carried out according to a previous study (35) with some modifications. Briefly, Mahlavu cells were grown to 70% to 80% confluence, washed with PBS, harvested with 5 mmol/L EDTA in PBS, and collected with serum-free medium containing 1% bovine serum albumin. Cell suspension was chilled at 4°C before adding 1.5×10^{11} plaque-forming units of phage-displayed peptide library. The reaction mixture was incubated at 4°C for 1 h, transferred to the top of a nonmiscible organic solvent (dibutyl phthalate/cyclohexane 9:1; Sigma-Aldrich), and centrifuged. The phage-bound cell pellet was resuspended with LB medium and the phages were amplified and titrated with *Escherichia coli* ER2738 culture (New England Biolabs). Recovered phages were subjected to additional rounds of biopanning with Mahlavu cells. The fifth-round phage elute was titrated on LB/IPTG/X-Gal plates for phage clone identification.

Identification of Phage Clones by ELISA

About 1×10^4 Mahlavu and NNM cells were seeded separately in 96-well ELISA plates and allowed to grow overnight. The plates were washed with serum-free DMEM and blocked with serum-free DMEM containing 1% bovine serum albumin at 4°C. Then, 10^9 plaque-forming units of individual phage clones were added and incubated at 4°C for 1 h. The plates were washed with PBS, and horseradish peroxidase–conjugated anti-M13 antibody (Amersham Biosciences) was added and incubated at 4°C for 1 h. The plates were washed with PBS followed by incubation with the peroxidase substrate *o*-phenylenediamine dihydrochloride (Sigma-Aldrich). The reaction was terminated by 3 N HCl, and absorbance was determined using a microplate reader at 490 nm.

DNA Sequencing and Computer Analysis

The phage DNA was extracted according to the manufacturer's instructions. The DNA sequences of purified phages were determined by dideoxynucleotide chain termination method using an automated DNA sequencer (ABI PRISM 377; Perkin-Elmer). The sequencing was done with the -96 gIII sequencing primer 5′-CCCTCATAGTTAGCGTAACG-3′. The phage-displayed peptide sequences were translated and aligned using a Genetic Computer Group program.

Flow Cytometry Analysis

Hepatocellular carcinoma cells were grown to 70% to 80% confluence and harvested with 5 mmol/L EDTA in PBS. Hepatocellular carcinoma cells were resuspended in fluorescence-activated cell sorting buffer (PBS with 1% fetal bovine serum) and incubated at 4°C for 1 h with PC94 or control phage, respectively. After washing with fluorescence-activated cell sorting buffer, hepatocellular carcinoma cells were incubated with monoclonal anti-M13 antibody at 4°C for 1 h followed by 30-min incubation with anti-mouse antibody conjugated to R-phycoerythrin (Southern Biotech). Analysis was done on FACSCalibur using CellQuest software (BD Bioscience).

Peptide Synthesis and Labeling

Targeting SP94 (SFSIIHTPILPL) and arbitrary control (FPWFPLPSPYGN) peptides were synthesized and purified by reverse-phase high-performance liquid chromatography to >95% purity by the Peptide Synthesis Core Facility, Institute of Biological Chemistry, Academia Sinica. Biotin-labeled peptides (biotin-SP94 and biotin-control-peptide) were synthesized by conjugating a biotin molecule to the peptide amino terminus. Mass spectrometry confirmed the predicted mass.

Animal Model for *In vivo* Targeting Assay

Severe combined immunodeficient mice (4-6 weeks old) were injected s.c. into the dorsolateral flank with 5×10^6 Mahlavu cells. Mice bearing Mahlavu-derived xenografts (500 mm^3) were injected i.v. with 2×10^9 plaque-forming units of PC94 or control phage. After perfusion, the organs (brain, heart, and lungs) and tumor tissue were removed, washed with cold PBS, and weighed. The phage bound to the tumor tissue and organs were rescued by *E. coli* ER2738 culture. The eluted phage particles were titrated on LB/IPTG/X-Gal plates. In peptide competitive inhibition experiments, 2×10^9 plaque-forming units of PC94 phage were coinjected with 100 μg SP94 peptide or the control peptide. The tissue distribution of targeting phages in the tumor-bearing mice was examined by immunohistochemical staining. The tissue sections were incubated with mouse anti-M13 antibody followed by incubation with biotinylated horse anti-mouse antibody (ABC kit; Vector Laboratories), washed with PBS, and then immersed with ABC reagent. The sections were immersed in 3,3′-diaminobenzidine solution plus 0.01% hydrogen peroxide, washed with PBS, and mounted with 50% glycerol in PBS.

For localization of the peptide-binding ability on liver cancer tissue, paraffin sections of human hepatocellular carcinoma were incubated with phage-displayed and biotin-labeled peptides using routine immunohistochemical procedures. The surgical specimens were obtained from the Tissue Bank of National Taiwan University Hospital with approval from the Institutional Review Board of National Taiwan University Hospital (IRB9461702021).

Preparation of Peptide-Liposomal Doxorubicin

The procedures for preparation of peptide-liposomal doxorubicin were described in our previous study (8, 33). Briefly, peptides were coupled to NHS-PEG-DSPE [*N*-hydroxysuccinimido-carboxyl-PEG (MW, 3400) derived distearoylphosphatidyl ethanolamine] in a 1:1.5 molar ratio. The coupling reaction was done with the free amine group in the amino terminus of the peptide to produce peptidyl-PEG-DSPE and confirmed by quantitation of the remaining amino groups with trinitrobenzenesulfonate reagent (Sigma-Aldrich). Peptidyl-PEG-DSPE was transferred to preformed PEGylated liposomal doxorubicin after coincubation at a temperature above the transition temperature of the lipid bilayer.

In vivo Tumor-Targeted Therapeutic Studies

Severe combined immunodeficient mice (4-6 weeks old) were injected s.c. into the dorsolateral flank with 5×10^6 Mahlavu cells. Tumor-bearing mice (100 mm^3) were then randomly assigned into four groups (six mice per group) for different treatments: A, SP94-Lipo-Dox (SP94-LD); B, Con-P-Lipo-Dox (CP-LD); C, Lipo-Dox (LD); and D, PBS. Treatments were administered through tail vein injection, 1 mg/kg twice a week, for 4 consecutive weeks, with a total dose of 8 mg/kg. In another experiment using mice bearing large Mahlavu-derived xenografts (550 mm^3), mice were also assigned into four groups as described. Treatments were administered through tail vein injection, 5 mg/kg once a week, for 2 consecutive weeks, with a total dose of 10 mg/kg. Body weights and the tumor sizes were measured by electronic scales and calipers. The tumor volumes were calculated using the equation: length × $(\text{width})^2 \times 0.52$. At the end of the experiment, tumor tissue and the visceral organs of each mouse were removed and fixed with 3% formaldehyde and OCT was embedded for further histopathologic examination. Animal care was carried out in accordance with guidelines of Academia Sinica.

Terminal Deoxynucleotidyl Transferase–Mediated dUTP Nick End Labeling Staining

The frozen tumor tissue sections were incubated with terminal deoxynucleotidyl transferase–mediated dUTP nick end labeling reaction mixture (Roche Diagnostics) at 37°C for 1 h. The slides were counterstained with Hoechst 33258 (Molecular Probes) and mounted with mounting medium (Vector Laboratories). Then, the slides were visualized under a fluorescent microscope.

CD31 Staining

The frozen tumor tissue sections were fixed with methanol/acetone (1:1), washed with PBS, and immersed in blocking buffer (1% bovine serum albumin in PBS) followed by incubation with rat anti-mouse CD31 (BD PharMingen). The sections were washed with $PBST_{0.1}$ (0.1% Tween 20 in PBS) and then incubated with rabbit anti-rat antibody (Stressgen) and immersed in rhodamine-labeled goat anti-rabbit antibody (Jackson ImmunoResearch). The slides were counterstained with Hoechst 33258, mounted with mounting medium, and visualized under a fluorescent microscope.

Total WBC Count

Blood was extracted from the submaxillary vein and mixed gently with 15% EDTA solution to prevent coagulation. RBC lysis buffer containing 2% acetic acid and 1% of Gentian violet (Sigma-Aldrich) was then added and

incubated at room temperature. The total WBC was calculated using a hemacytometer.

Results

Isolation of Phages Binding to Hepatocellular Carcinoma Cells

A phage-displayed random peptide library was used to isolate hepatocellular carcinoma, Mahlavu, cell-binding phages. After five rounds of affinity selection (biopanning), the recovery rate of the fifth round had increased 3.5-fold over that observed in the first round (Supplementary Fig. S1).[4] Ninety-six phage clones were randomly isolated and used to react with hepatocellular carcinoma cells and normal epithelial cells (NNM) by ELISA assay. Fifteen phage clones (PC1, PC2, PC9, PC12, PC15, PC26, PC42, PC47, PC62, PC72, PC84, PC85, PC86, PC88 and PC94) with higher hepatocellular carcinoma cell reactivity by ELISA (data not shown) and flow cytometry (Fig. 1A) were selected and sequenced. The phage-displayed peptide sequences were aligned by Genetic Computer Group software and revealed distinct consensus motif sequences (Table 1).

Identification of Phage Clones Specifically Binding to Hepatocellular Carcinoma Cells

To analyze the phage clones specifically binding to hepatocellular carcinoma cells, flow cytometry analysis was done. Hepatocellular carcinoma cells were incubated with each selected phage or control phage (Con-P). The surface-binding activity of each individual phage clone was analyzed by fluorescence-activated cell sorting. The results revealed that phage clone 94 (PC94) had the best reactivity to hepatocellular carcinoma cells, whereas the rest of the phage clones showed moderate binding activity to hepatocellular carcinoma cells (Fig. 1A). Based on the Genetic Computer Group alignment (Table 1), PC94 and PC88, both displaying the motif Pro-Ile/Leu-Leu-Pro (P-I/L-L-P), were selected for further study.

The binding activity of PC94 was further verified by incubating different dosages of phages with hepatocellular carcinoma cells and analysis by fluorescence-activated cell sorting. The results showed that the binding of PC94 to hepatocellular carcinoma cells occurs in a dose-dependent manner (Fig. 1B). In addition, no reactivity was found with the control helper phage or when PC94 was incubated with NNM (Fig. 1B). These results reveal that hepatocellular carcinoma Mahlavu cells express an unknown molecule that can be recognized by the peptide displayed on PC94.

To investigate whether other hepatocellular carcinoma cells can be recognized by PC94, nine hepatocellular carcinoma cell lines were incubated with PC94 and analyzed by fluorescence-activated cell sorting. The results show that six of nine hepatocellular carcinoma cell lines (Mahlavu, 59T, Hep3B, HepG2, NTUBL, and SKHep1) react strongly (47-81.2%) with PC94, whereas other hepatocellular carcinoma cell lines (Changliver and J5) have moderate reactivity (25.7-31.9%), and the HA22T cell line is only weakly reactive (19.1%; Fig. 1C). The binding specificity of PC94 for hepatocellular carcinoma cells was further tested using surgical specimens from hepatocellular carcinoma patients by immunohistochemistry. The results show that PC94 can recognize the tumor cells in surgical specimens of hepatocellular carcinoma (Fig. 1D, a and b) but not their normal counterparts (Fig. 1D, d). The control phage reveals no immunoreactivity in the tumor tissues of the hepatocellular carcinoma surgical specimens (Fig. 1D, c).

Animal Model for PC94 Targeting Study

To verify the targeting ability of PC94 *in vivo*, mice bearing Mahlavu-derived hepatocellular carcinoma xenografts (500 mm^3) were injected with PC94 or control phage through the tail vein. Phages circulated and were then perfused. Phage particles that bound to the tumor tissue and normal visceral organs were recovered. The results showed that significantly more PC94 phage particles were recovered (normalized per gram of tissue) from tumor tissue than from normal organs, such as brain (220-fold), heart (32-fold), and lungs (23-fold). However, the control phage revealed no homing phenomenon, neither in tumor tissue nor in normal organs (Fig. 2A).

The tumor-homing ability of PC94 was further confirmed by a peptide competitive inhibition experiment. Mice bearing hepatocellular carcinoma xenografts were coinjected with PC94 and the cognate synthetic peptide SP94. The results showed that SP94 markedly inhibited recovery of phage particle from tumor tissue. SP94 (100 μm) inhibited 88% of PC94 binding to tumor tissue, but the same concentration of a control peptide (Con-P) had no such inhibitory effect (Fig. 2B).

For verification of the tissue distribution of PC94, tissue sections of tumor and normal organs derived from the homing and competition experiments were immunostained by anti-phage antibody. It was found that only tumor cells revealed immunoreactivity (Fig. 2C, d and e) but not normal organs such as brain (Fig. 2C, a), heart (Fig. 2C, b), and lungs (Fig. 2C, c). However, when PC94 was coinjected with the cognate synthetic peptide SP94, no immunoreactivity was found in the tumor tissue (Fig. 2C, j). Neither tumor cells nor normal organs were found to have immunoreactivity with control phage (Fig. 2C, f-i).

Animal Model for Study of Ligand-Targeted Therapy

To evaluate the potential of SP94 as a targeting peptide that could improve the chemotherapeutic efficacy of anticancer therapy, we formulated a targeted DDS by coupling SP94 with PEGylated liposomal doxorubicin (SP94-LD). Mice bearing hepatocellular carcinoma xenografts (100 mm^3) were assigned into four groups for different treatments: A, SP94-LD; B, CP-LD; C, LD; and D, PBS. At the end of the treatment (day 28), the tumor size of the CP-LD and LD groups gradually increased to 1.5-fold larger than that of the SP94-LD group. The tumor size of the control PBS group was 3.3-fold larger than that of the SP94-LD group ($P < 0.01$; Fig. 3A). In addition, the group of tumor-bearing mice that received SP94-LD was found to have a lower tumor weight, ~40% inhibition compared

[4] Supplementary material for this article is available at Molecular Cancer Therapeutics Online (http://mct.aacrjournals.org/).

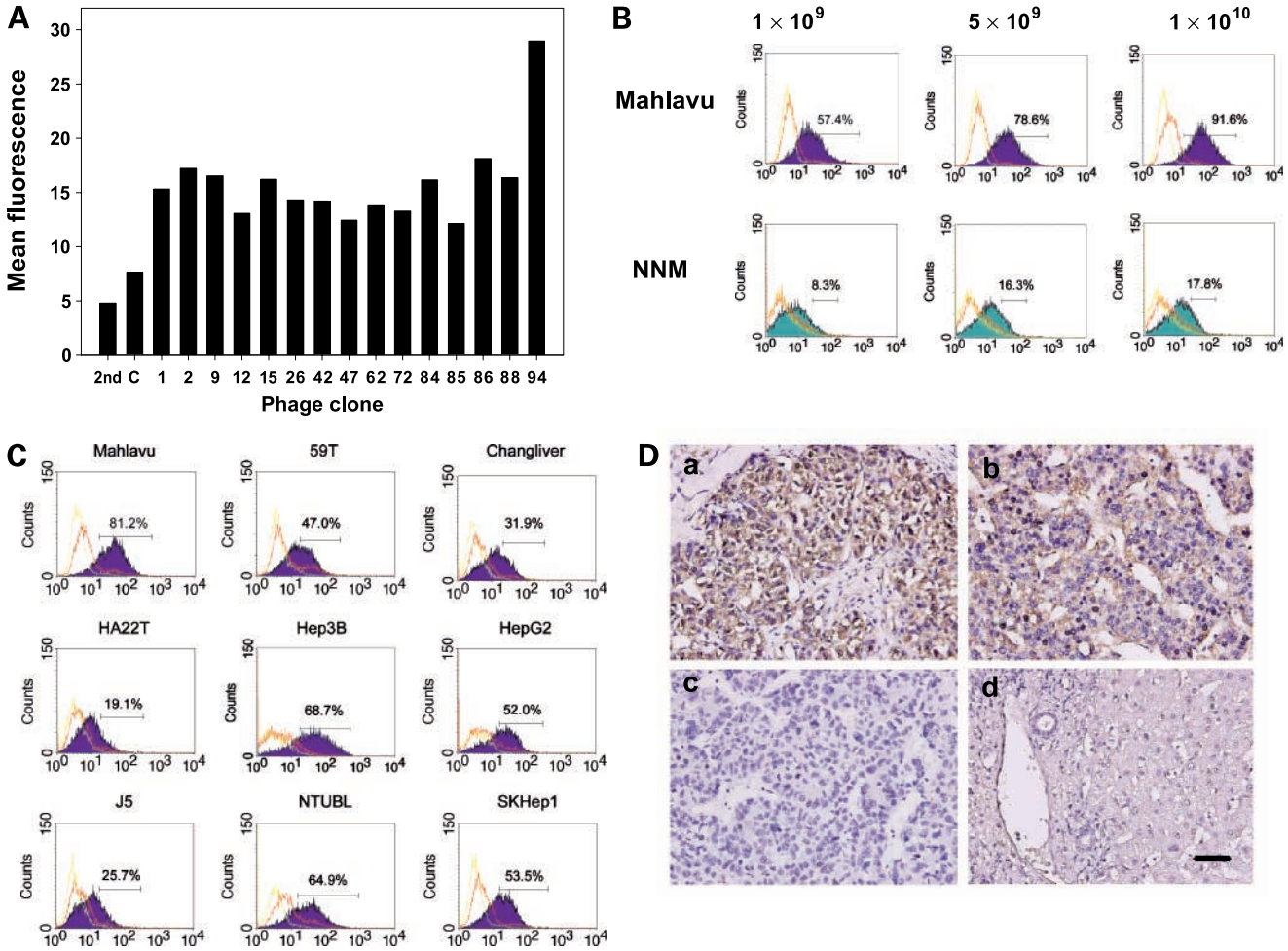

Figure 1. Binding activity of PC94 to hepatocellular carcinoma cell lines and human hepatocellular carcinoma biopsy specimens. **A,** surface-binding activity of each selected phage to hepatocellular carcinoma cells determined by flow cytometry (2nd, cells were stained with R-phycoerythrin-conjugated anti-mouse IgG; C, cells were incubated with control phage). **B,** dose-dependent binding activity of PC94 to hepatocellular carcinoma but not NNM cells. **C,** surface-binding activity of PC94 to each hepatocellular carcinoma cell line (yellow, staining with R-phycoerythrin-conjugated anti-mouse IgG; orange, cells incubated with control phage). **D,** biopsy specimens from hepatocellular carcinoma patients incubated with PC94 or control phage were detected using horseradish peroxidaseconjugated anti-M13 phage antibody. PC94 immunoreactivity was found in the tumor tissues (**a** and **b**) but not in their normal counterparts (**d**). Control phage could not bind to these biopsy specimens (**c**).

with that in the CP-LD- and LD-treated groups ($P < 0.01$; Fig. 3B).

To evaluate the side effects caused by the systemic delivery of chemotherapeutic drugs, the total WBC count was determined. The results revealed that the total WBC count of the SP94-LD-treated group ($1.9 \times 10^3/mm^3$) was higher than those of the CP-LD-treated ($1.6 \times 10^3/mm^3$) and LD-treated ($1.6 \times 10^3/mm^3$) groups but lower than that of the PBS group ($2.6 \times 10^3/mm^3$; Fig. 3C). The body weight did not significantly change in each treated group (Fig. 3D).

Histopathologic Examination and Immunofluorescent Detection of Tumor Blood Vessels and Apoptotic Cells in the Study of Ligand-Targeted Therapy

The histopathology of tumor tissues in each treatment group was examined by H&E staining. Marked disseminated necrotic/apoptotic areas were present throughout the whole section of SP94-LD-treated xenografts, whereas moderate amounts of necrotic/apoptotic areas were found in the LD- and CP-LD-treated xenografts. The PBS-treated group showed normal hepatocellular carcinoma cells (Fig. 4A). Terminal deoxynucleotidyl transferase–mediated dUTP nick end labeling was used to identify apoptotic cells, and anti-CD31 antibodies were applied to detect tumor blood vessels. Representative microscopic fields from the tumors show more apoptotic tumor cells (Fig. 4B) and a lower density of blood vessels (Fig. 4C) in the SP94-LD-treated group than in CP-LD- and LD-treated groups. Areas of $CD31^+$ endothelial cells were also quantified ($n = 6$) under low-power magnification. The amount of areas with $CD31^+$ endothelial cells was markedly decreased in the LD- and CP-LD-treated groups compared with those in the PBS group ($n = 6$; $P < 0.05$). Areas of $CD31^+$ endothelial cells

Table 1. Alignment of phage-displayed peptide sequences selected by Mahlavu cells

Phage clone	Phage-displayed peptide sequence*
94	SFSIIHT*PILP*L
88	ELMN*PLLP*FIQP
84	H*LP*STGNQYLSL
01	ETNWTHRP*PL*RV
15	EYRMAHL*TPSLL*
86	YHLQDSE*T*L*SLL*
42	SPWYMT*PSP*NTA
72	SVSVGMK*PSP*RP
47	DPMTWT*PS*SVMR
26	TPHRLDW*SP*HLV
02	GS*NP*W*N*TWLTTL
62	*NP*F*N*QHLHAQHP
09	S*ES*KDPTLWYPA
85	SFRLATP*ES*SRV
12	SNNEPMLRYTGQ

*Phage-displayed consensus amino acid sequences are italicized.

were fewer in the SP94-LD-treated group compared with those in CP-LD and LD groups ($n = 6$; $P < 0.001$; Fig. 4D). High tumor vascular density and no apoptotic cells were found in the PBS-treated group (Fig. 4B and C).

Ligand-Targeted Therapy for Treatment of Large Hepatocellular Carcinoma Xenograft Tumors

To verify whether large xenografts could also respond to SP94-LD treatment, mice bearing large hepatocellular carcinoma xenografts (550 mm^3) were assigned into four groups for different treatments. At the end of the treatment (day 14), the tumor sizes of the CP-LD and LD group gradually increased to 1.3- and 1.2-fold larger than that of the SP94-LD ($P = 0.089$ and $P < 0.05$, respectively). The tumor size of the control PBS group was 1.9-fold larger than that of the SP94-LD group ($P < 0.05$; Fig. 5A). In addition, the group of tumor-bearing mice that received SP94-LD was found to have a lower tumor weight than the CP-LD, LD, and PBS groups. The tumor weight of the CP-LD, LD, and PBS groups increased to 1.3-, 1.2-, and 2.1-fold larger than that of the SP94-LD group, respectively ($P < 0.05$; Fig. 5B). The total WBC count was also analyzed at day 10 and showed that the total WBC of the SP94-LD-treated group ($11.8 \times 10^3/mm^3$) was higher than those of the CP-LD-treated ($8.8 \times 10^3/mm^3$) and LD-treated ($8.2 \times 10^3/mm^3$) groups but lower than that of the PBS group ($13.9 \times 10^3/mm^3$; Fig. 5C).

The histopathology of tumor tissue in each treatment group was examined by H&E staining. Similarly, marked necrotic/apoptotic areas were present throughout the

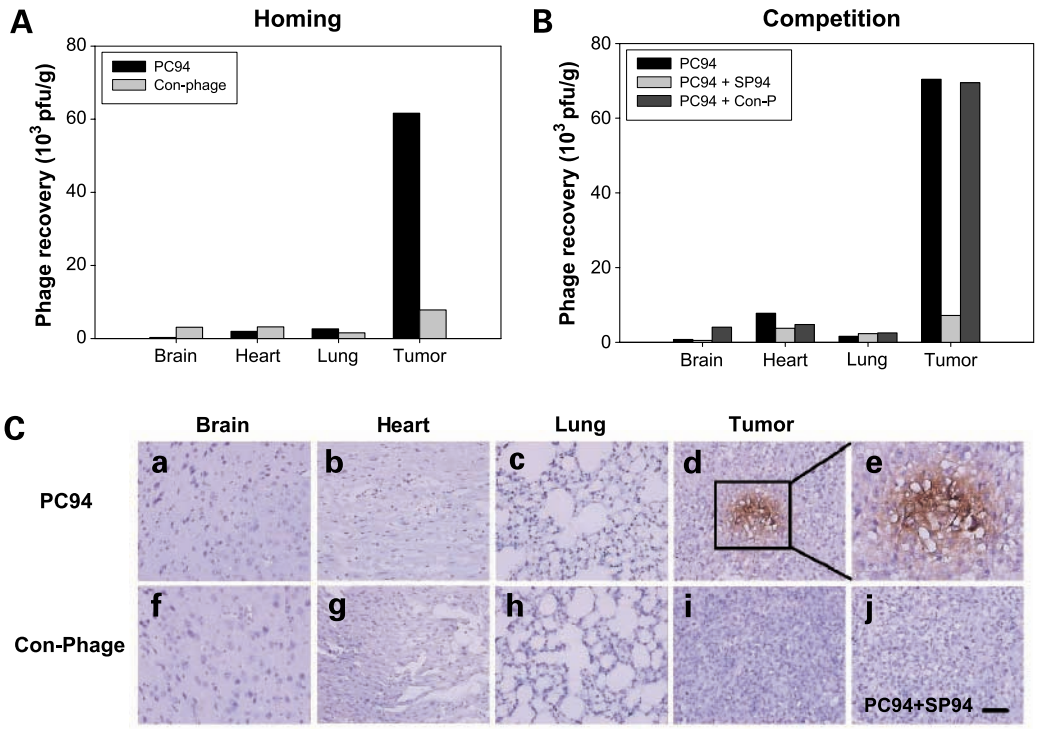

Figure 2. Verification of tumor-homing ability of PC94 *in vivo*. **A,** severe combined immunodeficient mice bearing hepatocellular carcinoma xenograft were injected i.v. with PC94, and phages were recovered after perfusion. The titer of PC94 recovered from the tumor was higher than that from visceral organs such as brain, heart, and lungs. **B,** targeting activity of PC94 to tumor tissues was competitively inhibited by SP94 but not by control peptides (Con-P). **C,** immunohistochemical detection of PC94 localization after i.v. injection into severe combined immunodeficient mice bearing hepatocellular carcinoma xenografts. Phage immunoreactivity localized in tumor tissues (**d** and **e**) but not in normal organs such as brain (**a**), heart (**b**), and lung (**c**) tissues or in the control phage-treated tumor section (**i**). The specific interaction of PC94 with the tumor section was inhibited by free peptide competition (**j**). Neither tumor cells nor normal organs were found to have immunoreactivity with control phage (**C, f-i**). Bar, 50 μm.

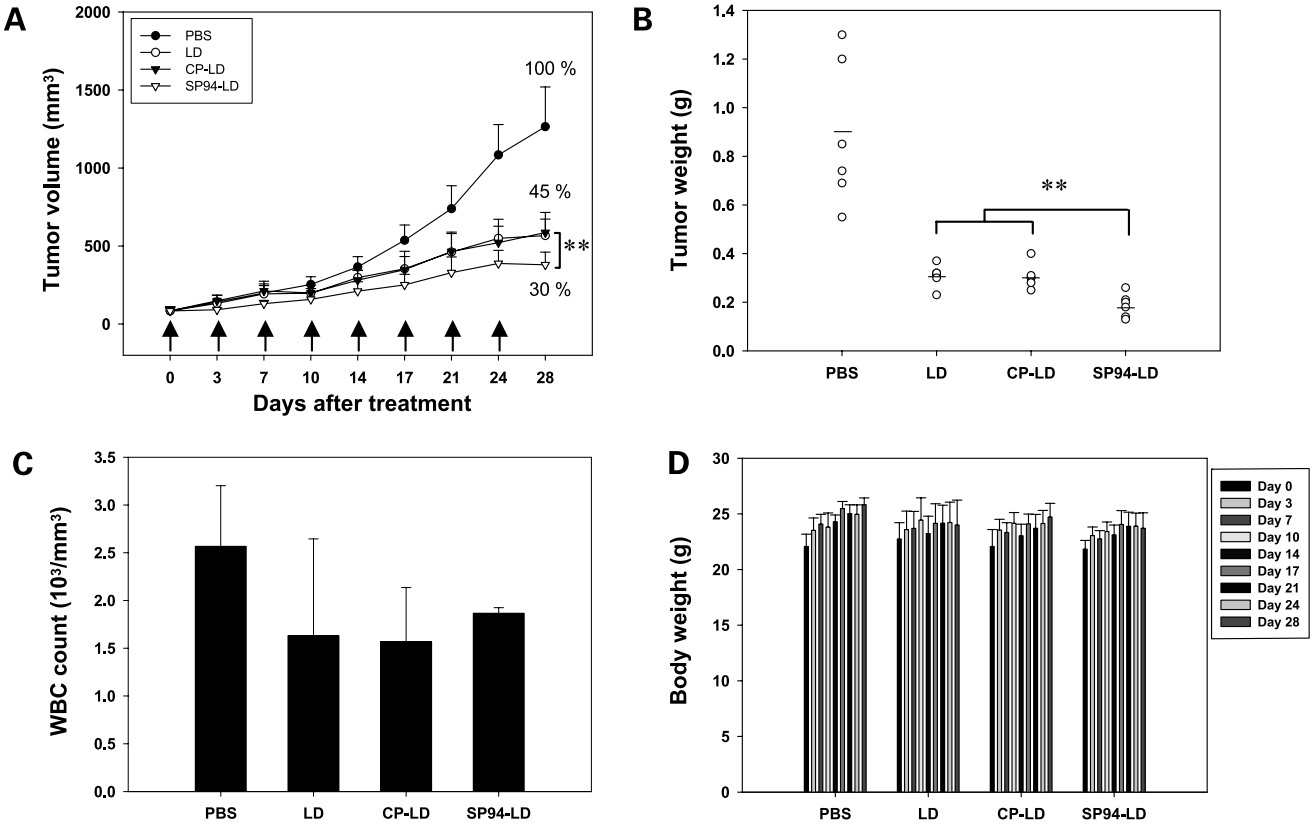

Figure 3. Conjugation of targeting peptide SP94 enhances the therapeutic efficacy and reduces the hematologic toxicity of liposomal doxorubicin in the hepatocellular carcinoma xenograft model. **A,** mice bearing hepatocellular carcinoma xenografts (100 mm^3) were injected i.v. with SP94-LD, CP-LD, LD, and PBS, respectively. The growth of tumor volume was markedly suppressed in the SP94-LD-treated group compared with that in the CP-LD and LD groups ($n = 6$). **, $P < 0.01$. **B,** at the end of treatment, tumor tissues were dissected and weighed. Tumor weight was lower in the SP94-LD-treated group compared with those in the CP-LD and LD groups ($n = 6$). **, $P < 0.01$. **C,** effect of different treatments on the WBC counts. **D,** body weight of each group. Bars, SE. *P* values were calculated by Student's *t* test.

whole sections from SP94-LD-treated xenografts, whereas moderate amounts of necrotic/apoptotic areas were found in the LD- and CP-LD-treated xenografts, and the PBS group showed normal hepatocellular carcinoma cells (Supplementary Fig. S2).[4] Areas of $CD31^+$ endothelial cells in the tumor tissues from each treatment were quantified ($n = 6$) under low-power magnification. The areas of $CD31^+$ endothelial cells were slightly fewer in the LD- and CP-LD-treated groups compared with those of the PBS group. However, areas of $CD31^+$ endothelial cells were significantly fewer in the SP94-LD-treated group compared with those in CP-LD and LD groups ($n = 6$; $P < 0.001$; Fig. 5D).

Discussion

Hepatocellular carcinoma is the fifth most common cancer and ranks as the fourth leading cause of cancer death worldwide (1). The only curative treatments are surgical resection or liver transplantation, but only a few patients are eligible for these procedures (36). The majority of hepatocellular carcinomas that present at an advanced stage are beyond curative treatment. Systemic chemotherapy against advanced hepatocellular carcinomas, either as single-agent therapy or in combination, has been investigated extensively in the past 30 years and is widely regarded as ineffective (36). How to improve the effectiveness of systemic treatment and select those patients who would benefit remains a major challenge. In this study, we report a novel targeting peptide identified via phage display screening and the development of ligand-targeted drug delivery against hepatocellular carcinoma.

A phage-displayed random peptide library was used to select hepatocellular carcinoma, Mahlavu, cell-specific phages. After five rounds of biopanning, ELISA screening and flow cytometry analysis were done to select phages able to bind to hepatocellular carcinoma cells. One phage clone named PC94, which had the best binding activity to hepatocellular carcinoma cells, was selected (Fig. 1A). To verify the binding ability of PC94 to other hepatocellular carcinoma cells, several hepatocellular carcinoma cell lines were investigated. The results show that all of these cell lines express the target molecule that can be recognized by the PC94-displayed peptide (Fig. 1C). Peptide competitive inhibition assay (Fig. 2) confirmed that the binding activity

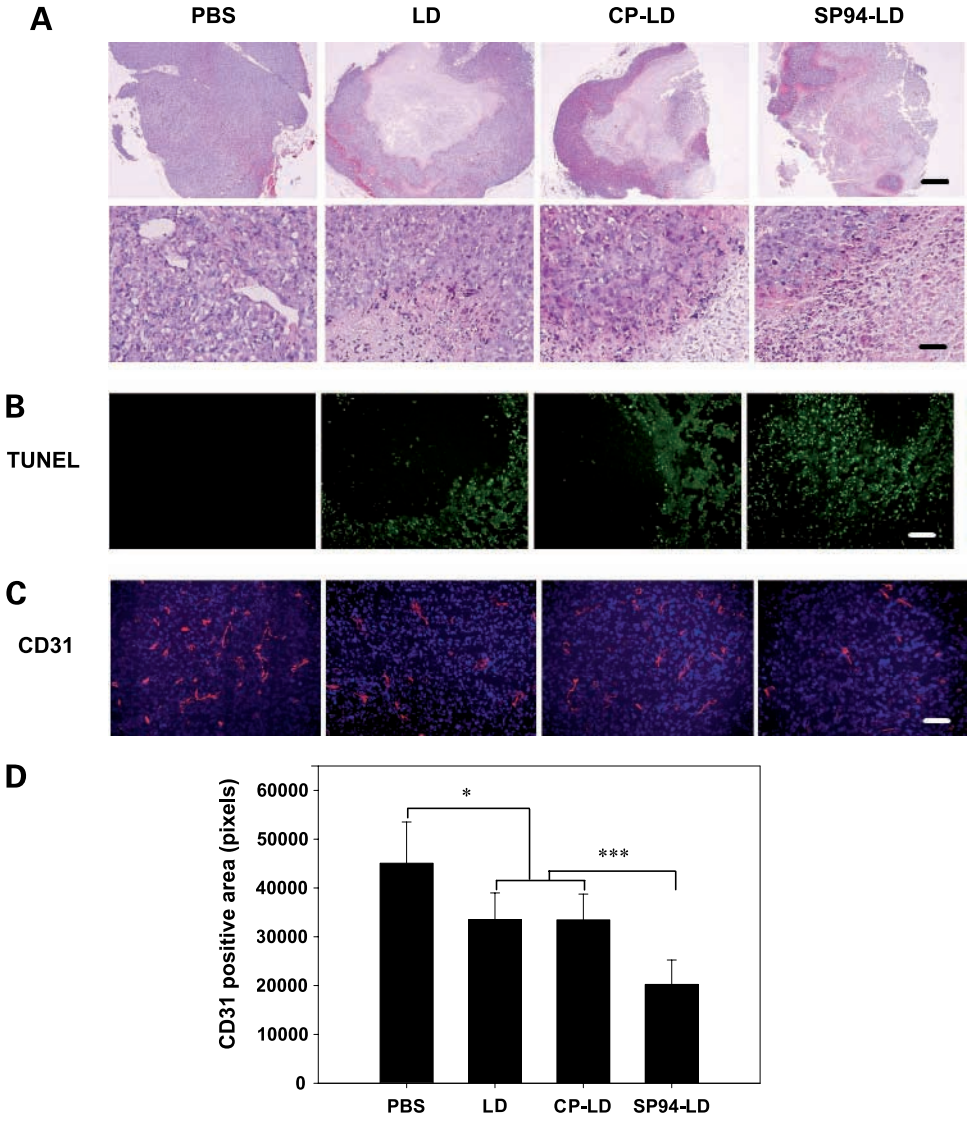

Figure 4. Histopathologic examination of SP94-LD-treated hepatocellular carcinoma xenografts. **A,** histopathology of tumor tissues of each treatment group examined after staining with H&E. The whole section of the SP94-LD-treated xenograft shows marked disseminated necrotic/apoptotic areas, whereas the CP-LD and LD xenografts reveal moderate necrotic/apoptotic areas and the PBS group shows normal hepatocellular carcinoma cells. Bar, 500 μm (*top*) and 50 μm (*bottom*). **B,** sections were terminal deoxynucleotidyl transferase–mediated dUTP nick end labeling labeled to visualize apoptotic tumor cells (*green*). The terminal deoxynucleotidyl transferase–mediated dUTP nick end labeling–positive tumor cells are distributed more evenly in the SP94-LD-treated group compared with in the CP-LD and LD groups. No apoptotic tumor cells were found in the PBS-treated group. Bar, 100 μm. **C,** sections were stained with anti-CD31 antibodies to visualize tumor blood vessels (*red*) and counterstained with H33258 (*blue*). Bar, 100 μm. Areas of $CD31^+$ endothelial cells were quantified ($n = 6$) at low-power magnification (**D**). The amounts of areas with $CD31^+$ endothelial cells are markedly decreased in the LD- and CP-LD-treated groups compared with those in the PBS group ($n = 6$). *, $P < 0.05$. The amounts of areas with $CD31^+$ endothelial cells are more reduced in the SP94-LD-treated group compared with those in the CP-LD and LD groups ($n = 6$). ***, $P < 0.001$. Bars, SE. P values were calculated by Student's t test.

of PC94 to hepatocellular carcinoma cells was dependent on the PC94-displayed peptide rather than another part of the phage particle. These results strongly suggest that the plasma membranes of these hepatocellular carcinoma cells express an unknown target molecule that can be recognized by both the synthetic peptide SP94 and the PC94-displayed peptide but not by other parts of the phage.

Several issues were addressed to evaluate the potential of SP94 as a drug delivery director for ligand-targeted drug delivery against hepatocellular carcinoma. First, we investigated whether SP94 could be targeted to hepatocellular carcinoma cells *in vivo*. For this, we examined the tumor-homing ability of PC94 and its competitive inhibition by SP94 in a hepatocellular carcinoma xenograft model. *In vivo* homing experiments showed that PC94 has homing ability to tumor tissues, with a binding activity >8-fold higher than that of the control phage (Fig. 2A). Moreover, in peptide competitive inhibition experiments, SP94 inhibited PC94 binding to the tumor mass, whereas the same concentration of a control peptide had no such inhibitory effect (Fig. 2B). To examine whether SP94 could increase the therapeutic index of targeted drugs, we investigated the binding specificity of SP94 to tumor tissues but not normal organs. In both the homing ability assay and the peptide competitive inhibition experiments, PC94 was found to bind specifically to tumor tissues but not to normal visceral organs, such as brain, heart, and lungs (Fig. 2A and B). Immunohistochemical staining showed that the PC94 particles were only localized in tumor tissues, but not in brain, heart, and lung tissues (Fig. 2C). Finally, we examined whether the SP94 ligand could recognize the target protein expressed by the tumor tissues of hepatocellular carcinoma patients. Both PC94 (Fig. 1D) and biotin-labeled SP94 (data not shown) recognized a target molecule produced on surgical specimens from hepatocellular carcinoma patients with a positive rate of 61.3% (19/31).

Taken together, we conclude that SP94 specifically recognizes an unknown target molecule expressed by hepatocellular carcinoma cells but not by normal tissues. This targeting ligand is therefore useful for developing targeted drug delivery against hepatocellular carcinoma.

The targeted DDS we developed includes three main components: (*a*) an anticancer drug, (*b*) a carrier, and (c) targeting ligands. Because doxorubicin has been reported to provide the most consistent overall response rate (18%) in hepatocellular carcinoma (36) and liposomal doxorubicin has also been shown to have remarkable activities in refractory breast and ovarian cancers (37, 38), this drug was chosen as the anticancer agent and PEG-coated liposome (PEGylated liposome) was chosen as the carrier. PEGylated liposomal doxorubicin was coupled with targeting ligand SP94 (SP94-LD) to assess the efficacy of targeted drug delivery against hepatocellular carcinoma. In the human hepatocellular carcinoma xenograft model, SP94-LD showed an improvement in therapeutic efficacy compared with control peptide conjugated LD-treated (CP-LD) and LD-treated groups (Figs. 3 and 5).

Without being bound by any particular mechanism, the partial inhibition of tumor growth of CP-LD- and LD-treated groups may be accounted for by the following factors. First, the leakiness of the angiogenic tumor vasculature may allow selective extravasation of drug conjugates in tumor tissue. In addition, drug conjugates may be retained in tumor tissue due to the lack of an effective lymphatic drainage. These factors result in passive targeting and accumulation of the drug conjugates in tumor tissue (14). It has also been shown in animal studies that long-circulating PEGylated liposomal doxorubicin leads to passive preferential localization in tumors and results in a several-fold increase of drug concentration in the tumor relative to that obtained with free drugs (15, 39). Using a combination of SP94 and PEGylated liposomal doxorubicin, a process called active or ligand-mediated targeting, the site-specific actions of this targeted DDS further enhanced the antitumor effects (Figs. 3 and 5) through increased tumor apoptosis (Fig. 4A and B; Supplementary Fig. S2)[4] and decreased tumor angiogenesis (Figs. 4C and 5D).

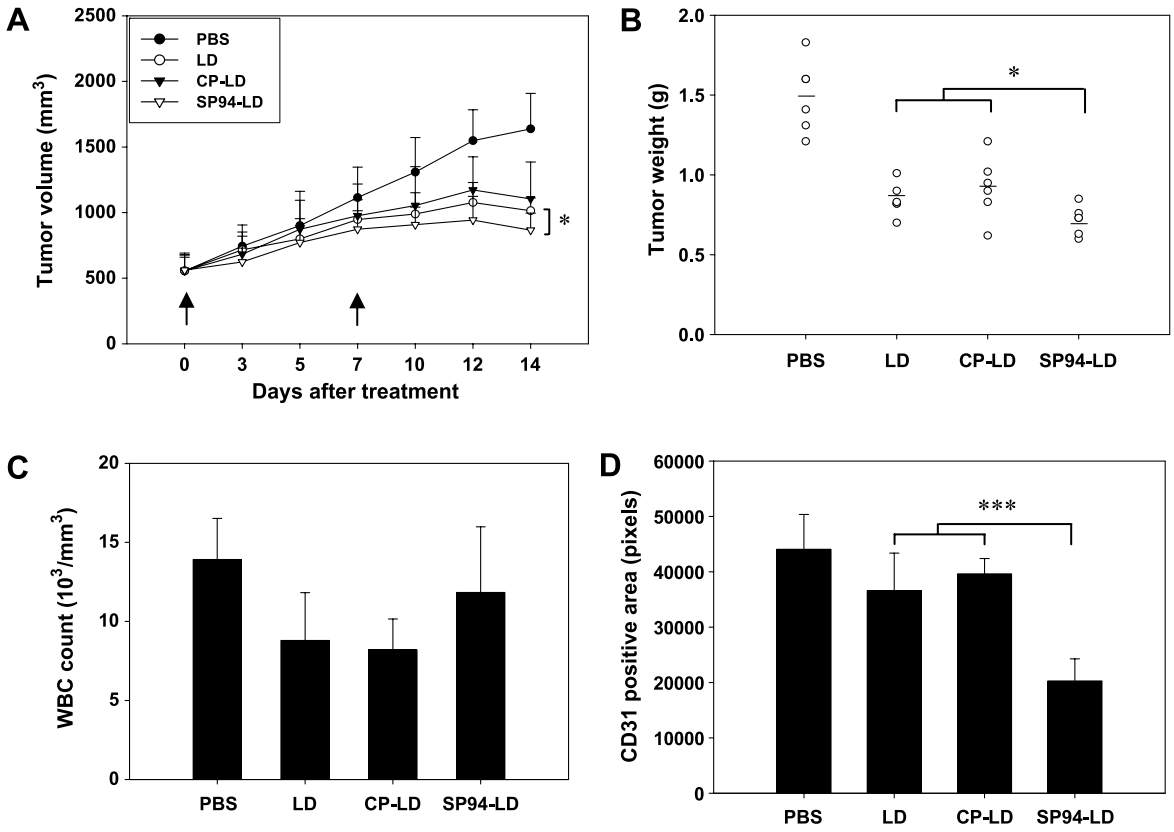

Figure 5. Treatment of severe combined immunodeficient mice bearing large hepatocellular carcinoma xenografts with SP94-LD. **A,** mice bearing large hepatocellular carcinoma xenografts (550 mm^3) were injected i.v. with SP94-LD, CP-LD, LD, and PBS, respectively. The tumor growth is markedly suppressed in the SP94-LD-treated group compared with that in CP-LD and LD groups ($n = 6$). *, $P < 0.05$. **B,** after treatments had finished, tumor masses were dissected and weighed. The tumor weight is lower in the SP94-LD-treated group compared with that in the CP-LD and LD groups ($n = 6$). *, $P < 0.05$. **C,** effect of different treatments on the WBC counts. **D,** amounts of areas with $CD31^+$ endothelial cells are slightly decreased in the LD- and CP-LD-treated groups compared with those in the PBS group. The amounts of areas with $CD31^+$ endothelial cells are significantly reduced in the SP94-LD-treated group compared with those in the CP-LD and LD groups ($n = 6$). ***, $P < 0.001$. Bars, SE. P values were calculated by Student's t test.

In clinical trials of formulations of PEGylated liposomal doxorubicin, improved pharmacokinetic properties and reduced systemic toxicity have been shown (40). Here, our results revealed that with the site-specific actions of this targeted DDS, SP94-LD can further decrease hematologic toxicities by avoiding the reduction in the total WBC (Figs. 3C and 5C). The reduction in the total WBC count observed with nontargeted PEGylated liposomal doxorubicin (CP-LD and LD) may be due to the increased circulation time of the drug, its confinement in blood vessels, and the increased chances of its nonspecific uptake by mononuclear phagocytic system cells. Such leukopenia has already been reported in a phase II clinical trial of PEGylated liposomal doxorubicin for patients with advanced hepatocellular carcinoma (41, 42).

Some previous studies of the phase II clinical trial of PEGylated liposomal doxorubicin have reported that the drug exhibited almost no activity in advanced hepatocellular carcinoma, with response rates of 0% to 14% at best (41–43). The enhanced therapeutic efficacy of SP94-LD described here therefore indicates significant clinical potential for this targeted DDS in the treatment of advanced hepatocellular carcinoma patients. Identification of the target molecule interacting with SP94 would enable verification of its specific expression on hepatocellular carcinoma tumor tissue and authenticate its use as a target for hepatocellular carcinoma therapy.

In conclusion, we used a phage-displayed peptide library to identify a novel peptide SP94, which can specifically bind to the hepatocellular carcinoma cell surface both *in vitro* and *in vivo*. In addition, PC94 recognized the tumor tissue surface but not normal counterparts in surgical specimens from hepatocellular carcinoma patients. Conjugation of the targeting peptide SP94 and liposomes containing doxorubicin improved therapeutic efficacy in a hepatocellular carcinoma xenograft model. The SP94 peptide thus has significant clinical potential to improve the systemic treatment of advanced hepatocellular carcinomas.

Acknowledgments

We thank Dr. Yun-Long Tseng for preparation of liposome complex and Mary Wyatt for reading the article.

References

1. Thomas MB, Zhu AX. Hepatocellular carcinoma: the need for progress. J Clin Oncol 2005;23:2892–9.

2. Farazi PA, DePinho RA. Hepatocellular carcinoma pathogenesis: from genes to environment. Nature Rev 2006;6:674–87.

3. Jemal A, Murray T, Ward E, et al. Cancer statistics, 2005. CA Cancer J Clin 2005;55:10–30.

4. Bosslet K, Straub R, Blumrich M, et al. Elucidation of the mechanism enabling tumor selective prodrug monotherapy. Cancer Research 1998; 58:1195–201.

5. Allen TM, Cullis PR. Drug delivery systems: entering the mainstream. Science 2004;303:1818–22.

6. Allen TM, Mumbengegwi DR, Charrois GJ. Anti-CD19-targeted liposomal doxorubicin improves the therapeutic efficacy in murine B-cell lymphoma and ameliorates the toxicity of liposomes with varying drug release rates. Clin Cancer Res 2005;11:3567–73.

7. MacDiarmid JA, Mugridge NB, Weiss JC, et al. Bacterially derived 400 nm particles for encapsulation and cancer cell targeting of chemotherapeutics. Cancer Cell 2007;11:431–45.

8. Lee TY, Wu HC, Tseng YL, Lin CT. A novel peptide specifically binding to nasopharyngeal carcinoma for targeted drug delivery. Cancer Res 2004; 64:8002–8.

9. Xiong XB, Huang Y, Lu WL, et al. Enhanced intracellular delivery and improved antitumor efficacy of doxorubicin by sterically stabilized liposomes modified with a synthetic RGD mimetic. J Control Release 2005; 107:262–75.

10. Vasey PA, Kaye SB, Morrison R, et al. Phase I clinical and pharmacokinetic study of PK1 [*N*-(2-hydroxypropyl)methacrylamide copolymer doxorubicin]: first member of a new class of chemotherapeutic agents-drug-polymer conjugates. Cancer Research Campaign Phase I/II Committee. Clin Cancer Res 1999;5:83–94.

11. Duncan R. The dawning era of polymer therapeutics. Nat Rev Drug Discov 2003;2:347–60.

12. Satchi-Fainaro R, Mamluk R, Wang L, et al. Inhibition of vessel permeability by TNP-470 and its polymer conjugate, caplostatin. Cancer Cell 2005;7:251–61.

13. Hashizume H, Baluk P, Morikawa S, et al. Openings between defective endothelial cells explain tumor vessel leakiness. Am J Pathol 2000;156:1363–80.

14. Matsumura Y, Maeda H. A new concept for macromolecular therapeutics in cancer chemotherapy: mechanism of tumoritropic accumulation of proteins and the antitumor agent smancs. Cancer Res 1986; 46:6387–92.

15. Northfelt DW, Martin FJ, Working P, et al. Doxorubicin encapsulated in liposomes containing surface-bound polyethylene glycol: pharmacokinetics, tumor localization, and safety in patients with AIDS-related Kaposi's sarcoma. J Clin Pharmacol 1996;36:55–63.

16. Papahadjopoulos D, Allen TM, Gabizon A, et al. Sterically stabilized liposomes: improvements in pharmacokinetics and antitumor therapeutic efficacy. Proc Natl Acad Sci U S A 1991;88:11460–4.

17. Northfelt DW, Dezube BJ, Thommes JA, et al. Pegylated-liposomal doxorubicin versus doxorubicin, bleomycin, and vincristine in the treatment of AIDS-related Kaposi's sarcoma: results of a randomized phase III clinical trial. J Clin Oncol 1998;16:2445–51.

18. Stewart S, Jablonowski H, Goebel FD, et al. Randomized comparative trial of pegylated liposomal doxorubicin versus bleomycin and vincristine in the treatment of AIDS-related Kaposi's sarcoma. International Pegylated Liposomal Doxorubicin Study Group. J Clin Oncol 1998;16:683–91.

19. Harrington KJ, Mohammadtaghi S, Uster PS, et al. Effective targeting of solid tumors in patients with locally advanced cancers by radiolabeled pegylated liposomes. Clin Cancer Res 2001;7:243–54.

20. Al-Batran SE, Bischoff J, von Minckwitz G, et al. The clinical benefit of pegylated liposomal doxorubicin in patients with metastatic breast cancer previously treated with conventional anthracyclines: a multicentre phase II trial. Br J Cancer 2006;94:1615–20.

21. Wu HC, Chang DK, Huang CT. Targeted therapy for cancer. J Cancer Mol 2006;2:57–66.

22. Jain RK. Transport of molecules in the tumor interstitium: a review. Cancer Res 1987;47:3039–51.

23. Willett CG, Boucher Y, di Tomaso E, et al. Direct evidence that the VEGF-specific antibody bevacizumab has antivascular effects in human rectal cancer. Nat Med 2004;10:145–7.

24. Mori T. Cancer-specific ligands identified from screening of peptide-display libraries. Curr Pharmaceutical Design 2004;10:2335–43.

25. Chen YC, Huang HN, Lin CT, Chen YF, King CC, Wu HC. Generation and characterization of monoclonal antibodies against dengue virus type 1 for epitope mapping and serological detection by epitope-based peptide antigens. Clin Vaccine Immunol 2007;14:404–11.

26. Liu IJ, Hsueh PR, Lin CT, et al. Disease-specific B Cell epitopes for serum antibodies from patients with severe acute respiratory syndrome (SARS) and serologic detection of SARS antibodies by epitope-based peptide antigens. J Infect Dis 2004;190:797–809.

27. Wu HC, Jung MY, Chiu CY, et al. Identification of a dengue virus type 2 (DEN-2) serotype-specific B-cell epitope and detection of DEN-2-immunized animal serum samples using an epitope-based peptide antigen. J Gen Virol 2003;84:2771–9.

28. Shadidi M, Sioud M. Identification of novel carrier peptides for the specific delivery of therapeutics into cancer cells. FASEB J 2003;17:256–8.

29. Zitzmann S, Mier W, Schad A, et al. A new prostate carcinoma binding peptide (DUP-1) for tumor imaging and therapy. Clin Cancer Res 2005;11:139 – 46.

30. Arap W, Pasqualini R, Ruoslahti E. Cancer treatment by targeted drug delivery to tumor vasculature in a mouse model. Science 1998;279: 377 – 80.

31. Hoffman JA, Giraudo E, Singh M, et al. Progressive vascular changes in a transgenic mouse model of squamous cell carcinoma. Cancer Cell 2003;4:383 – 91.

32. Joyce JA, Laakkonen P, Bernasconi M, Bergers G, Ruoslahti E, Hanahan D. Stage-specific vascular markers revealed by phage display in a mouse model of pancreatic islet tumorigenesis. Cancer Cell 2003;4: 393 – 403.

33. Lee TY, Lin CT, Kuo SY, K. CD, Wu HC. Peptide-mediated targeting to tumor blood vessels of lung cancer for drug delivery. Cancer Res 2007;67: 10958 – 65.

34. Pastorino F, Brignole C, Di Paolo D, et al. Targeting liposomal chemotherapy via both tumor cell-specific and tumor vasculature-specific ligands potentiates therapeutic efficacy. Cancer Res 2006;66:10073 – 82.

35. Giordano RJ, Cardo-Vila M, Lahdenranta J, Pasqualini R, Arap W. Biopanning and rapid analysis of selective interactive ligands. Nat Med 2001;7:1249 – 53.

36. Burroughs A, Hochhauser D, Meyer T. Systemic treatment and liver transplantation for hepatocellular carcinoma: two ends of the therapeutic spectrum. Lancet Oncol 2004;5:409 – 18.

37. Muggia FM, Hainsworth JD, Jeffers S, et al. Phase II study of liposomal doxorubicin in refractory ovarian cancer: antitumor activity and toxicity modification by liposomal encapsulation. J Clin Oncol 1997;15: 987 – 93.

38. Ranson MR, Carmichael J, O'Byrne K, Stewart S, Smith D, Howell A. Treatment of advanced breast cancer with sterically stabilized liposomal doxorubicin: results of a multicenter phase II trial. J Clin Oncol 1997;15: 3185 – 91.

39. Hong RL, Huang CJ, Tseng YL, et al. Direct comparison of liposomal doxorubicin with or without polyethylene glycol coating in C-26 tumor-bearing mice: is surface coating with polyethylene glycol beneficial? Clin Cancer Res 1999;5:3645 – 52.

40. Hong RL, Tseng YL. Phase I and pharmacokinetic study of a stable, polyethylene-glycolated liposomal doxorubicin in patients with solid tumors: the relation between pharmacokinetic property and toxicity. Cancer 2001;91:1826 – 33.

41. Hong RL, Tseng YL. A phase II and pharmacokinetic study of pegylated liposomal doxorubicin in patients with advanced hepatocellular carcinoma. Cancer Chemother Pharmacol 2003;51:433 – 8.

42. Valle JW, Dangoor A, Beech J, et al. Treatment of inoperable hepatocellular carcinoma with pegylated liposomal doxorubicin (PLD): results of a phase II study. Br J Cancer 2005;92:628 – 30.

43. Schmidinger M, Wenzel C, Locker GJ, et al. Pilot study with pegylated liposomal doxorubicin for advanced or unresectable hepatocellular carcinoma. Br J Cancer 2001;85:1850 – 2.

Molecular Cancer Therapeutics

Hepatocellular carcinoma cell-specific peptide ligand for targeted drug delivery

Albert Lo, Chin-Tarng Lin and Han-Chung Wu

Mol Cancer Ther 2008;7:579-589.